

obtained when a Lorentzian form factor was assumed for the bonding charge. The model which provides the best fit is one based on a tetrahedral distortion of the outer electronic shells, and an ionic charge transfer from In to Sb. A similar model was proposed a few years ago for interpreting x-ray data in diamond, silicon, and germanium.^{13,14} The basic idea is that the charge density of the valence electrons can be expanded in a series of cubic harmonics, in such a way that the overall symmetry of the nonspherical charge density is that of the atomic sites. We have extended this model to the Zn-Se structure by introducing an ionic charge transfer between two nearest neighbors, so that the charge density at any point in the crystal is expressed by means of spherically symmetric Hartree-Fock wave functions and two adjustable parameters. One of them, α , controls the amount of tetrahedral distortion, and the other one, λ , regulates an ionic charge transfer. Our analysis shows that this model provides an excellent fit with experiment, with an R factor more than an order of magnitude smaller than that obtained from the bond-charge model.

Measurements taken at various temperatures between 400 and 16°K indicate that the amount of charge transfer and tetrahedral distortion vary slightly with temperature. These results at different temperatures, along with a description of

the experiments and model calculations presented above, will be reported with greater detail in a forthcoming article.

*Research supported by the National Science Foundation—Materials Research Laboratory Grant No. GH-33574A1 and by National Science Foundation Grant No. GH-39200.

¹P. P. Ewald and H. Hönl, *Ann. Phys. (Leipzig)* **25**, 281 (1936).

²R. Brill, *Acta Crystallogr.* **13**, 275 (1960).

³J. C. Phillips, *Phys. Rev.* **166**, 832 (1968).

⁴J. C. Phillips, *Covalent Bonding in Crystals, Molecules and Polymers* (Univ. of Chicago Press, Chicago, Ill., 1969), pp. 35, 67–74, 160.

⁵J. P. Walter and M. L. Cohen, *Phys. Rev. B* **4**, 1877 (1971).

⁶Y. W. Yang and P. Coppens, *Solid State Commun.* **15**, 1555 (1974).

⁷R. Colella, *Phys. Rev. B* **3**, 4308 (1971).

⁸The dislocation density evaluated by etch-pit count was about 15/cm².

⁹B. Dawson and B. T. M. Willis, *Proc. Roy. Soc., London, Ser. A* **298**, 307 (1967).

¹⁰J. P. Walter, private communication.

¹¹Equations 2.84 and 4.80 of Ref. 4.

¹²Equation 2.24 of Ref. 4.

¹³B. Dawson, *Proc. Roy. Soc., London, Ser. A* **298**, 264 (1967).

¹⁴R. J. Weiss, *X-Ray Determination of Electron Distributions* (Wiley, New York, 1966), pp. 64–67, 139–141.

Photoelectron Spin Polarization Testing the Ionic Structure of 3d Levels in Ferrites

S. F. Alvarado, W. Eib, and H. C. Siegmann

Laboratorium für Festkörperphysik, Eidgenössische Technische Hochschule, CH-8049 Zurich, Switzerland

and

J. P. Remeika

Bell Laboratories, Murray Hill, New Jersey 07974

(Received 14 July 1975)

The dependence of photoelectron spin polarization on photon energy with ultrahigh-vacuum-cleaved surfaces of several ferrites shows that the electronic excitation spectrum of 3d states is described by the model of a single ion in a crystal field in all details. We obtain the relative intensity of the multiplet lines as well as the energy difference of 3dⁿ⁻¹ final states on A- and B-lattice sites with high precision.

At present, photoemission of electrons emerges as a handle on the old problem of whether the 3d states in a solid might be treated in analogy to the 4f shell by the model of a single ion in a crystal field (SICF). If this model applies, the structure in the energy distribution curves (EDC's) of

photoelectrons emitted from 3dⁿ shells arises from the spectrum of the hole left behind and not from an initial band density of states. Support for this interpretation has been recently provided by photoemission spectra obtained with x-ray¹ and uv-photon energies. However, even in the

most simple cases like MnO, where the two single lines are resolved,² it turns out that the relative line intensity deviates by a factor of 2 or more from theoretical predictions. The question arises whether this discrepancy reveals an inadequacy of the SICF model. We give experimental evidence that the SICF model describes the electronic excitation spectra of transition-metal ions in ferrites and oxides accurately. It turns out that the measurement of electron spin polarization (ESP) in photoemission can be made a *differential method* comparing the line intensities with high precision, without the need to analyze the kinetic energy of photoelectrons.

Consider first the simple case where a $3d^5$ shell (Fe^{3+}) is located in a cubic crystal field. By photoemission of one electron, the spherical symmetric 6A_1 configuration goes into one of the two possible configurations of $3d^4$, namely 5E or 5T_2 , which are well separated by the crystal-field splitting $10Dq = \Delta$; see Sugano, Tanabe, and Kani-mura.³ The ratio η of the two transitions should be 1 according to the coefficients of fractional parentage. Suppose further that Fe^{3+} is located in the cubic spinel crystal structure, which has a tetrahedral A site and an octahedral B site. Although the magnitude of the crystal field is almost equal on A and B sites, $\Delta_B/\Delta_A = 1.125$,⁴ the sign is opposite. It follows that while 5E is the ground state of $3d^4$ on the B site, on the A site the ground state is 5T_2 . Figure 1 shows an idealized EDC of photoelectrons expected with a ferrite containing Fe^{3+} only. Indicated on each line is the state in which the ion core is left behind. The line shape with a width Δ_n at half-maximum accounts for the finite lifetime of the ion core and apparatus resolution. The total emission strength from the A sites is proportional to $1 - \delta$, and from B sites to $1 + \delta$, where $1 - \delta$ and $1 + \delta$ are the respective densities of Fe^{3+} on the two sites. The initial state and relaxation energies at the A and B sites might be different. This is accounted for by ΔE .

The EDC $N(E)$ in Fig. 1 is idealized also because the effect of escape over the surface-barrier potentials and of inelastic scattering has been omitted. In the ferrites, the work function Φ is ~ 6.5 eV so that production of secondary electrons is impossible up to photon energies $\hbar\omega \leq 13$ eV. Furthermore, the band gap between oxygen $2p$ bands and Fe $4s$ bands is probably ~ 5 eV,⁵ and it is likely that even inelastic electron-electron scattering is very weak at $\hbar\omega \lesssim 10$ eV for the same reasons that have been found to apply to

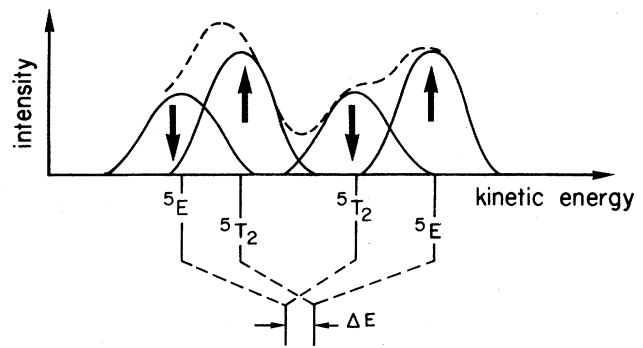


FIG. 1. Idealized photoelectron EDC's expected from a ferrite containing Fe^{3+} ($3d^5$) only. The ions at B sites emit up-spin electrons only (\dagger); the A sites, down-spin electrons (\ddagger). Indicated below each peak is the state in which the ion core Fe^{4+} ($3d^4$) is left behind. The center of gravity of $3d^4$ can be different by ΔE on A and B sites. The dashed line is the sum of the A - and B -site contributions that would be observed in an experiment with energy analysis if there were neither inelastic-scattering effects nor effects of escape over the surface-barrier potentials.

EuO .⁶ Inelastic scattering can therefore be neglected at low $\hbar\omega$. This has the additional desirable effect that the mean free path of photoexcited electrons is large and one tests bulk properties. The effect of the surface barrier is accounted for by the escape probability S . If the kinetic energy $E < \Phi$, $S = 0$; and for $E > \Phi$, $S = 1 - \exp[-(E - \Phi)/k]$. The constant k is of the order of 1–2 eV.⁶ A more realistic EDC is then $N(E)S(E)$. The spin polarization comes in because the B lattice emits up-spin electrons only (intensity i^\dagger) and the A lattice down-spin electrons (i^\ddagger). This arises because A and B sites are coupled antiferromagnetically. The ESP is given by $P = (i^\dagger - i^\ddagger)/(i^\dagger + i^\ddagger)$ with $i^\dagger = \int N_B(E)S(E)dE$ and $i^\ddagger = \int N_A(E) \times S(E)dE$. One can guess without any numerical calculations from Fig. 1 that $P(\hbar\omega)$ will be strongly dependent upon those parameters that introduce differences in the yield of electrons from A sites relative to B sites, like η or ΔE , but not upon those affecting the yield on both sublattices in the same way, such as Δm or k .

Photoelectron-spin-polarization measurements were performed by the Mott-scattering technique; clean surfaces were obtained by cleaving single crystals in ultrahigh vacuum (2×10^{-10} Torr). A magnetic field of 16 kG to align the Weiss domains was applied perpendicular to the photoemitting surfaces, and the crystals were also at $\sim 60^\circ\text{K}$. Results have been obtained with Mg_2 -

$(\text{Fe}^{3+})_{1-\delta}[\text{Mg}_{1-\delta}(\text{Fe}^{3+})_{1-\delta}]\text{O}_4$ (magnesium ferrite), $\text{Ni}_{0.5}\text{Zn}_{0.5}\text{Fe}_2\text{O}_4$ (nickel zinc ferrite), and, as already reported,⁷ Fe_3O_4 (magnetite) and $\text{Fe}^{3+}[\text{Li}_{0.5}(\text{Fe}^{3+})_{2.5}]\text{O}_4$ (lithium ferrite). The ions in brackets are at *B* sites. Magnesium ferrite is the ideal material to test the SICF model: (i) It contains Fe^{3+} only; (ii) the strong crystal field leads to a large line separation²; and (iii) δ can be varied, $0 \leq \delta \leq 0.3$, by heat treatment of the samples. Since the magnetization is $M = 2\delta\mu_{\text{Fe}^{3+}}$, with $\mu_{\text{Fe}^{3+}} = 5\mu_B$, one has a full range of materials from an *A-B* antiferromagnet ($\delta = 0$) to a ferrimagnet with high M . Figure 2 shows, as one example, the results of a measurement on magnesium ferrite with $\delta = 0.24$. In a large range of $\hbar\omega$, there is an excellent agreement between the $P(\hbar\omega)$ calculated from the SICF model and the observed ESP. Note that the *absolute* value of $P(\hbar\omega)$ must agree; i.e., no background can be subtracted! With one and the same set of the five parameters η , ΔE , Δ_B , Δm , and k one can fit all the $P(\hbar\omega)$ curves measured on ten magnesium ferrite surfaces with different values of δ . We obtain $\eta = 1.00 \pm 0.02$, $\Delta E = 0.00 \pm 0.05$ eV, $\Delta_B = 2.0 \pm 0.2$ eV, $\Delta m \sim 0.5$ eV, and $k \sim 1.5$ eV. The main effect of k and Δm is to smear the structure at $\hbar\omega \sim 9$ eV. From the fact that this peak is clearly resolved, one obtains upper limits $\Delta m \leq 0.8$ eV, or $k \leq 3$ eV. These con-

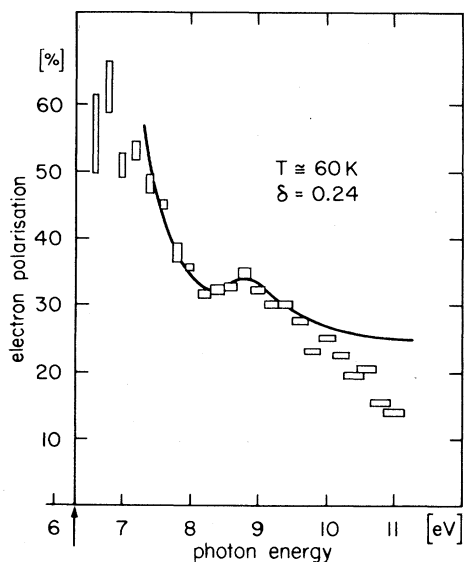


FIG. 2. Photoelectron spin polarization with magnesium ferrite as a function of photon energy $\hbar\omega$ at constant magnetic field $H = 16$ kG. The solid line was calculated from the SICF model. The arrow indicates photoelectric threshold.

stants affecting the yield of electrons from both sublattices are not accurately determined as expected. Two significant deviations from the experimental and calculated ESP curves are observed in all the magnesium ferrite (and also the lithium ferrite): Near threshold and for $\hbar\omega > 10$ eV the observed ESP is too low. The deviations for $\hbar\omega$ near Φ can be attributed to photoemission from unpolarized impurity states lying in the forbidden energy zone. The square root of the photoelectric yield, $Y^{1/2}$, plotted versus $\hbar\omega$ exhibits a tail which shows that such states are actually present. The deviations at $\hbar\omega \geq 10$ eV are most likely due to the onset of emission from the unpolarized oxygen bands.

The following further observations show that the SICF model is universal in understanding the electronic excitation spectra of ferrites.

(1) Lithium ferrite is similar to magnesium ferrite in that it has Fe^{3+} only at *A* and *B* sites. $P(\hbar\omega)$ calculated with η , k , and Δm the same as in magnesium ferrite but $\Delta E = 0.25 \pm 0.05$ eV and $\Delta_B = 1.5 \pm 0.1$ eV fits the measurements⁸ in a perfect way.

(2) If the initial state is not $3d^5$, the initial- and final-state multiplets become numerous. From a $3d^6$ (Fe^{2+}) initial state, one can reach seven different excited states of $3d^5$. Therefore, seven plus four from Fe^{3+} at *A* and *B* sites which is eleven lines are squeezed into an energy range of less than 3 eV in magnetite. The multiplets can never be resolved because the inherent linewidth is ~ 0.5 eV. The same holds for nickel zinc ferrite. This is why the applicability of the SICF model has not been realized so far. Earlier EDC's with magnetite taken by Bishop and Kemeny⁹ and also the ESP experiment⁷ have been interpreted on the basis of one-electron energy levels generated by crystal-field-split $3d$ bands.¹⁰ That such models do not apply is unambiguously seen only from the measurement on magnesium ferrite, where a $3d^5$ level, unsplit by the cubic crystal field, generates a double structure (observe Fig. 2). But one can explain the spectra of magnetite and nickel zinc ferrite by the SICF model in a very natural way.¹¹ In magnetite for instance, one peak is resolved near threshold, and the ESP is negative. This must be assigned to emission of a minority spin from Fe^{2+} on a *B* site leaving behind the Fe^{3+} -ion core in its ground state 6A_1 configuration. 6A_1 has a large energy separation from the rest of the lines because of minimum exchange energy. The convincing argument is that the SICF model explains the electron-

ic excitation spectra of all ferrites with only two adjustable parameters Δ_B and ΔE , since the linewidth Δm and k , which may be different in the various ferrites which range from metals to insulators, does not enter the ESP data critically.

This is one of the few cases in which a simple model explains data obtained by photoemission in a quantitative way.

We are indebted to M. Campagna for very helpful discussions and suggestions and to the Schweizerischer Nationalfonds for supporting this work.

¹G. K. Wertheim, H. J. Guggenheim, and S. Hüfner, *Phys. Rev. Lett.* **30**, 1050 (1973).

²D. E. Eastman and J. L. Freeouf, *Phys. Rev. Lett.*

34, 395 (1975).

³S. Sugano, Y. Tanabe, and M. Kanimura, *Multiplets of Transition Metal Ions in Crystals* (Academic, New York, 1970).

⁴A. Herpin, *Théorie du Magnétisme* (Presses Universitaires de France, Paris, 1968), p. 142.

⁵D. Adler, *J. Solid State Chem.* **12**, 332 (1975).

⁶D. E. Eastman, *Phys. Rev. B* **8**, 6027 (1973).

⁷S. F. Alvarado, W. Eib, F. Meier, D. T. Pierce, H. C. Siegmann, and J. P. Remeika, *Phys. Rev. Lett.* **34**, 319 (1975).

⁸D. E. Eastman, *Techniques of Metals Research* (Interscience, New York, 1972), Vol VI.

⁹S. G. Bishop and P. C. Kemeny, *Solid State Commun.* **15**, 1877 (1974).

¹⁰D. L. Camphausen, J. M. D. Coey, and B. K. Chakraverty, *Phys. Rev. Lett.* **29**, 657 (1972), and references cited therein.

¹¹A full description of this work is being prepared.

$L_{2,3}$ Transitions in Liquid Na and Al: Edge Singularity and Extended X-Ray-Absorption Fine Structure

H. Petersen and C. Kunz

Deutsches Elektronen-Synchrotron DESY, 2000 Hamburg 52, Germany

(Received 8 May 1975)

The $L_{2,3}$ excitation spectra of liquid and solid Na and Al were measured at several temperatures throughout the energy intervals 30–80 and 70–170 eV, respectively, using yield spectroscopy. The spike at the 31-eV Na edge is virtually unchanged in the liquid, indicating that the edge is insensitive to long-ranged crystalline order. The broader structures up to 100 eV above the edges in Na and Al, however, are washed out in the liquid.

Recently considerable theoretical effort has been devoted to the interpretation of the photoabsorption spectra of electrons initially orbiting in the $2p$ core levels of simple metals; one-electron theories offer competing explanations of structures both at the $L_{2,3}$ thresholds and as much as 100 eV above.

At the $L_{2,3}$ edges, the threshold spikes seemed to be well explained by the many-body theory of Mahan¹ and Nozières and De Dominicis,² which attributed the observed spikes to the shielding of the core hole by conduction electrons. However, the same theory also predicted the rounding of K edges and contained a parity selection rule which led to predictions of conspicuous dependence of edge shapes upon momentum transfer³ in x-ray Raman scattering or electron energy-loss scattering. Dow and co-workers⁴ have disagreed with the many-body explanation of the Li K -edge rounding and have proposed a phonon

core-level broadening mechanism to explain the edge shape. We have recently observed thermal broadening in the region of the absorption threshold.^{5,6} Tests of the many-body theory's selection rule by Sonntag⁷ (in $\text{Li}_{1-x}\text{Cu}_x$ alloys) and by Ritsko, Schnatterly, and Gibbons⁸ (using electron energy loss) did not produce the predicted changes of the Li edge shape. From these and other facts,⁹ questions arise concerning the limitation of the many-body theory. Nevertheless the spike at the Na $L_{2,3}$ edge still provides an outstanding experimental support of this theory. Unlike similar, though weaker, features at the $L_{2,3}$ edges of Mg and Al the spike in Na cannot be easily dismissed as a density-of-states structure. Its behavior upon melting should provide valuable clues to its origin and to its dependence on long-ranged crystalline order.

The spectral region well above the $L_{2,3}$ edges is the subject of yet another theoretical dispute